Original Article

Macular Imaging Characteristics in Children with Myelinated Retinal Nerve Fiber and High Myopia Syndrome

Almila Sarıgül Sezenöz*, Sibel Oto*, İmren Akkoyun*, Sezin Akça Bayar*, Gürsel Yılmaz*, Meriç Yavuz Çolak**

*Başkent University Faculty of Medicine, Department of Ophthalmology, Ankara, Türkiye
**Başkent University Faculty of Medicine, Department of Biostatistics, Ankara, Türkiye

Abstract

Objectives: To investigate the macular imaging features in patients with unilateral myelinated retinal nerve fiber (MRNF) and high myopia syndrome.

Materials and Methods: Six patients with unilateral MRNF and high myopia syndrome and 13 myopic controls were enrolled in this study. Spectral domain (SD) optical coherence tomography (OCT), SD enhanced depth imaging OCT, and OCT angiography (OCTA) imaging results of MRNF-affected eyes were compared with the fellow eyes and myopic controls.

Results: All patients had abnormal foveal reflex and/or ectopia. No significant difference in retinal thickness parameters were noted between the groups. In OCT scans, posterior vitreous detachment (PVD) was observed in 4 out of the 6 MRNF-affected eyes. Regarding OCTA parameters, only a significant increase in acircularity index was noted in myelinated eyes (p=0.01).

Conclusion: All patients demonstrated normal foveal contours, macular structure, and OCTA features except for a higher acircularity index. The incidence of PVD was notably increased in the myelinated eyes.

Keywords: Myelinated retinal nerve fiber, high myopia, optical coherence tomography, optical coherence tomography angiography

Cite this article as: Sarıgül Sezenöz A, Oto S, Akkoyun İ, Akça Bayar S, Yılmaz G, Çolak MY. Macular Imaging Characteristics in Children with Myelinated Retinal Nerve Fiber and High Myopia Syndrome. Turk J Ophthalmol 2023;53:234-240

Address for Correspondence: Almila Sarıgül Sezenöz, Başkent University Faculty of Medicine, Department of Ophthalmology, Ankara, Türkiye
E-mail: almilasarigul@gmail.com **ORCID-ID:** orcid.org/0000-0002-7030-5454
Received: 02.06.2022 **Accepted:** 05.01.2023

DOI: 10.4274/tjo.galenos.2023.27612

Introduction

Myelinated retinal nerve fiber (MRNF) is a developmental anomaly appearing as gray-white striated patches corresponding in shape to the distribution of the retinal nerve fiber layer (RNFL).[1,2] The syndrome of unilateral heavy MRNF surrounding mainly the superior temporal arcade, hypoplastic/dysplastic optic disc, and high myopia is a separate entity from incidental MRNF patches.[2]

The visual prognosis of amblyopia associated with MRNF and anisomyopia is reported to be poorer than that of anisomyopic amblyopia without MRNF.[3,4,5,6,7] Macular involvement of MRNF has been reported in a few cases, but the macula usually appears normal in patients with optic nerve dysplasia.[1,3,8,9]

Optical coherence tomography (OCT) is a non-invasive tool that can be used for cross-sectional imaging of the chorioretinal layers. Case studies have reported the macular spectral domain (SD)-OCT findings of MRNF. While some studies reported normal foveal morphology, others reported increased RNFL thickness, anatomic distortion of the macular region, macular pseudohole formation, and attenuation of the photoreceptor integrity line.[2,10,11,12,13]

OCT angiography (OCTA) evaluates the microvasculature of the retinochoroidal layers and allows quantitative evaluation of blood flow by several vascular metrics such as vessel density (VD), acircularity index (AI), and foveal avascular zone (FAZ).[14,15] Only one case series consisting of two patients reported the influence of localized MRNF on peripapillary VD in OCTA.[16] To the best of our knowledge, there are no published reports outlining macular OCTA findings in MRNF and high myopia syndrome.

We investigated the clinical and imaging features of unilateral MRNF, high myopia, and amblyopia syndrome and compared the macular SD-OCT, enhanced depth imaging (EDI)-OCT, and OCTA imaging characteristics with normal fellow eyes and a myopic control group.

Materials and Methods

The study protocol was approved by the local ethics committee of Başkent University. The medical records of patients diagnosed with unilateral MRNF, myopic anisometropia, and amblyopia at the Başkent University Department of Ophthalmology and followed in our clinic since 2001 were reviewed. Those with at least one OCT and OCTA image during follow-up were included in the patient group. These patients' unaffected contralateral eyes and the right eyes of otherwise healthy patients with high myopia (≥-6.00 diopters [D]) and normal fundus appearance were included as controls. Exclusion criteria for both the patient and control groups were the presence of significant media opacities that would interfere with good-quality image capture; any additional retinal and systemic vascular diseases; any optic nerve diseases; other macular pathologies such as macular edema, macular scar, or epiretinal membrane; dome-shaped macula; and any ocular trauma or intraocular surgical history.

Written informed consent to participate in the study was obtained from all subjects. The age, spherical equivalent (SE), and best corrected visual acuity (BCVA) of the patient at the time of OCT and OCTA imaging was considered for the analyses.

A full ophthalmologic examination was performed for all patients. Macular OCT was performed with the Heidelberg Spectralis OCT ART 1 20x20º program and the choroid was visualized with SD-EDI-OCT (Spectralis, Heidelberg Engineering, Heidelberg, Germany). The EDI-OCT mode uses eye tracking technology to take 50 images and generates high-resolution B-mode scans from these images. Subfoveal choroidal thickness (SCT) was defined as the vertical distance from the outer portion of the hyperreflective line corresponding to the retinal pigment epithelium/Bruch's membrane complex to the hyperreflective line on the inner surface of the sclera and was measured by the manual caliper function of the software. For retinal thickness measurements, SD-OCT (Spectralis; Heidelberg Engineering) was used. The retinal thickness maps were created automatically by the software, which identified the vitreoretinal interface and retinal pigment epithelium/choriocapillaris as regions of high reflectance. The software is designed to quantify retinal thickness as the separation of these boundaries in micrometers at fixation and as the average value for each of 9 different areas, including the central 1 mm.[17] The images were obtained between 10:00 and 11:00 AM to eliminate diurnal fluctuations in choroidal thickness.

OCTA images were obtained by AngioVue OCT (Optovue Inc., Fremont, CA, USA). The AngioAnalytics software of the OptoVue system, which contains an automated segmentation algorithm, was used to assess superficial and deep VD in the macular 6x6 mm region and in the perifoveal region, as well as the FAZ area in square millimeters (mm^2). The percentage of total area occupied by blood vessels was recorded as the VD value. The boundary of the superficial capillary plexus was defined from 3 µm below the internal limiting membrane to 15 µm below the inner plexiform layer. The boundary of the deep capillary plexus was defined from 15 to 70 µm below the inner plexiform layer. VD (%) was quantified automatically by the built-in software of the OCT system. The software automatically fits a circle 1.0 mm in diameter centered on the fovea. The parafoveal region is defined as a 2.0-mm-wide annulus around the fovea, and the perifoveal region is defined as a 3.0-mm-wide annulus around the parafovea.[18] The AngioVue System provides signal strength index values in order to define the image quality based on the intensity or brightness of the reflected light during scanning.[19] OCTA images with scan quality ≥5 were included for analysis. The whole-image macular, perifoveal, parafoveal, and foveal VDs of the superficial and deep capillary plexuses were calculated automatically by the built-in software of the OCTA device. The FAZ area in the full retinal vasculature (mm^2) and the AI were also calculated automatically via the FAZ assessment tool. The AI of the FAZ is calculated by dividing the perimeter of the FAZ by the perimeter of a circle with equal area. A perfectly circular FAZ has an AI of 1.0, and an increase in this metric indicates deviation from the circular shape of the FAZ.[20]

The OCT and OCTA images of patients with MRNF and high myopia syndrome were compared with images of their normal contralateral eyes and 13 myopic controls.

Statistical Analysis

The IBM Statistics Package for the Social Sciences version 23.0 (IBM Corp., Armonk, NY, USA) was used for the analysis. Descriptive statistics were used to summarize the data. Analytical evaluations were made to compare the groups. Kruskal-Wallis analysis of variance was used to compare the data of the three groups. For the variables that had significant differences within the groups, a Bonferroni-adjusted Mann-Whitney U test was performed. In statistical analysis, the value $p<0.05$ was considered significant. In post-hoc comparisons, the Bonferroni-adjusted alpha value was taken as 0.017.

Results

Six patients (4 males, 2 females) with unilateral MRNF, myopic anisometropia, and amblyopia and 13 otherwise healthy myopic controls (5 males, 8 females) were enrolled.

The mean age of the patient group was 11.88±3.77 years (range: 5.5-15.8 years) and that of the myopic control group was 11.81±4.67 years (range: 6-21 years) (p=0.83). The mean SE of the myelinated eyes was -12.21±4.44 D (range: -7.00 to -17.50 D), that of the normal eyes was -0.92±2.56 D (range: +1.50 to -5.00 D) and that of the myopic control group was -8.97±2.08 D (range: -6.00 to -12.75 D). SE values were compared between the two independent groups (myelinated eyes and myopic control subjects) using the non-parametric Mann-Whitney U test and found to be statistically similar (p=0.11). The median

axial length (AL) of the patients' myelinated eyes was 27.95 mm (range: 26.43 to 30.66 mm) and that of the myopic control group was 26.43 mm (range: 24.58 to 28.40 mm), with no statistically significant difference between the groups (p=0.09). Table 1 shows the AL, central retinal thickness (CRT), and SCT measurement results of all groups.

All patients showed optic disc hypoplasia, abnormal macular reflex, and/or foveal displacement. In five patients, the fovea in the myelinated eye was below the horizontal line going through the inferior margin of the optic disc (Figure 1). All patients showed ocular deviation in their myelinated eyes and were given occlusion therapy based on the visual acuity difference between eyes and the presence and amount of deviation. The mean BCVA of the myelinated eyes was 0.87±0.58 logMAR (range: 0.30-1.80 logMAR) at the first visit and 0.51±0.66 logMAR (range: 0.00-1.80 logMAR) at the last visit. The mean follow-up time was 80.55±55.94 months.

OCT images of the 6 MRNF and high myopia syndrome patients and 13 myopic control patients were obtained (Figure 2). The median CRT was 272.00 µm (interquartile range [IQR]=152.50) in myelinated eyes, 258.50 µm (IQR=19.25) in contralateral normal eyes, and 258.00 µm (IQR=41.50) in the myopic controls, with no significant difference within the groups (p=0.51). The median SCT was 159.00 µm (IQR=169.50) in myelinated eyes, 263.00 µm (IQR=94.00) in contralateral normal eyes, and 206.5 µm (IQR=102.50) in the myopic control group, with no significant difference between the groups (p=0.09). Comparison of perifoveal retinal thicknesses among the groups is shown in Table 2. There was no significant difference in retinal thicknesses in any quadrants. Macular OCT images revealed posterior vitreous detachment (PVD) in the myelinated eye in 4 out of 6 patients (Figure 3). None of the normal fellow eyes or myopic controls had PVD.

OCTA images were successfully obtained from both eyes of 4 patients with MRNF and high myopia syndrome and all 13 myopic controls (Figure 4). OCTA features including AI, flow area, FAZ, and VD of the superficial and deep layers were noted (Table 3). Only AI differed significantly among the three groups in the Kruskal-Wallis test (p=0.02). Bonferroni-adjusted Mann-Whitney U tests with an adjusted alpha value of 0.017 showed that only the difference between myelinated eyes and the high myopia control group was statistically significant, with higher AI in myelinated eyes (p=0.003). There were no statistically significant differences in pairwise comparisons of mean AI values between myelinated eyes and normal fellow eyes or between normal fellow eyes and the myopic control group (p=0.03 and p=0.55, respectively).

Discussion

In this study, the foveal structure in MRNF and high myopia syndrome was investigated by SD-OCT, EDI-OCT, and OCTA

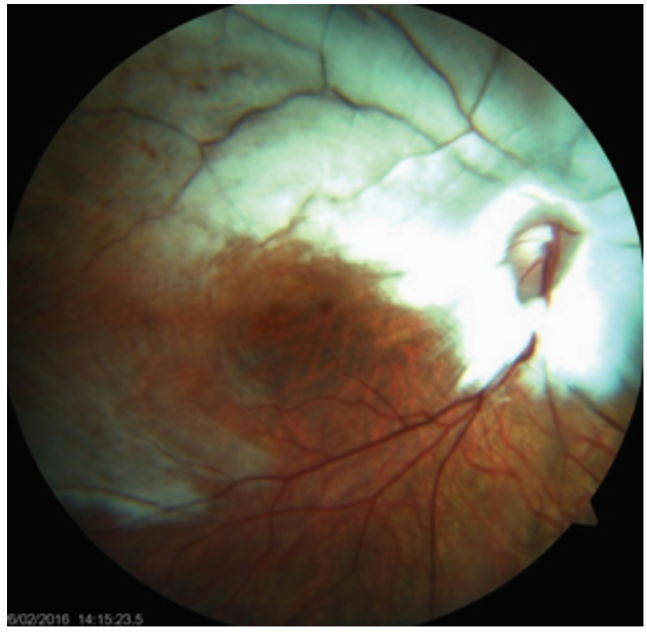

Figure 1. Fundus photograph of the myelinated eye of a patient with unilateral myelinated retinal nerve fiber and high myopia syndrome

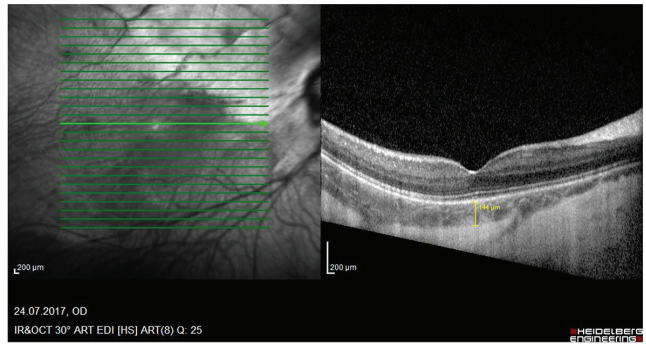

Figure 2. Macular enhanced depth imaging optical coherence tomography image of a patient with myelinated retinal nerve fiber and high myopia with inferior foveal displacement, showing the measurement of subfoveal choroidal thickness

Table 1. The axial length, central retinal thickness and subfoveal choroidal thickness results of myelinated eyes, normal fellow eyes, and the myopic control group

	Myelinated eyes, median (IQR)	Normal fellow eyes, median (IQR)	Myopic controls, median (IQR)	p*
Axial length (mm)	27.95 (3.19)	24.33 (1.46)	26.43 (2.15)	0.01
Central retinal thickness (µm)	272.00 (152.50)	258.50 (19.25)	258.00 (41.50)	0.51
Subfoveal choroidal thickness (µm)	159.00 (169.50)	263.00 (94.00)	206.5 (102.50)	0.09

IQR: Interquartile range (Q3–Q1), *The p values are for the comparison of the three groups with Kruskal–Wallis test.

Table 2. Comparison of perifoveal retinal thickness in 8 surrounding quadrants (EDTRS fields) and macular volume of myelinated eyes, normal fellow eyes, and the myopic control group

	Myelinated eyes, median (min-max) (IQR) (n=6)	Normal fellow eyes, median (min-max) (IQR) (n=6)	Myopic controls, median (min-max) (IQR) (n=13)	p
Temporal inner ring (µm)	342.00 (265.00-404.00) (87.25)	318.50 (315.00-322.00) (4.00)	316.00 (282.00-437.00) (29.00)	0.71
Superior inner ring (µm)	342.00 (129.00-467.00) (147.50)	334.00 (326.00-349.00) (12.50)	333.00 (279.00-436.00) (16.50)	0.96
Nasal inner ring (µm)	339.50 (307.00-368.00) (53.5)	331.00 (326.00-349.00) (5.00)	331.00 (296.00-422.00) (21.50)	0.98
Inferior inner ring (µm)	324.00 (159.00-387.00) (64.25)	332.50 (327.00-336.00) (7.50)	336.00 (291.00-445.00) (20.00)	0.81
Temporal outer ring (µm)	301.00 (265.00-400.00) (132.00)	283.50 (275.00-300.00) (18.25)	290.00 (237.00-418.00) (48.00)	0.93
Superior outer ring (µm)	339.00 (103.00-483.00) (245.00)	296.00 (295.00-303.00) (2.75)	300.00 (237.00-395.00) (28.00)	0.91
Nasal outer ring (µm)	293.50 (35.00-366.00) (183.25)	315.00 (302.00-330.00) (20.50)	314.00 (262.00-386.00) (24.00)	0.62
Inferior outer ring (µm)	285.50 (229.00-390.00) (65.75)	292.50 (271.00-308.00) (16.75)	289.00 (245.00-426.00) (75.50)	0.89
Macular volume (μm^3)	8.83 (6.85-11.35) (3.04)	8.57 (8.33-8.82) (0.19)	8.67 (7.23-11.39) (0.93)	0.80

IQR: Interquartile range (Q3-Q1), min: Minimum, max: Maximum

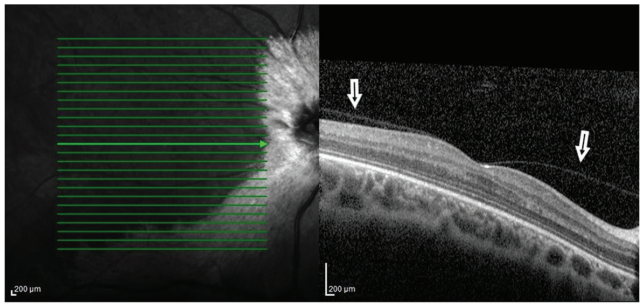

Figure 3. Macular enhanced depth imaging optical coherence tomography image of a patient with myelinated retinal nerve fiber and high myopia showing partial posterior vitreous detachment (arrows)

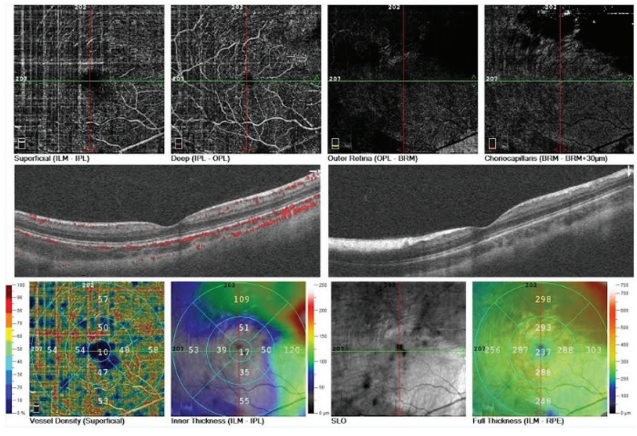

Figure 4. Macular optical coherence tomography angiography image of a patient with unilateral myelinated retinal nerve fiber and high myopia syndrome

to determine if there is a structural etiology that may explain the poorer visual prognosis of the affected eye. All patients demonstrated normal foveal contours, macular structure, and OCTA features except for a higher AI. The incidence of PVD was notably increased in the myelinated eyes.

Normal myelination in the visual pathway starts at 32 weeks of gestation from the lateral geniculate body and stops at the lamina cribrosa.[21] Local factors within the lamina cribrosa act as a barrier and prevent oligodendrocyte migration and intraretinal myelination of retinal ganglion cell axons.[22,23] Widespread MRNFs are usually associated with higher degrees of axial myopia.[24,25] Oh et al.[26] found a strong association between localized scleral excavation and the distribution of MRNF, suggesting that the local visual deprivation caused by MRNF induces focal scleral excavation and contributes to the development of axial myopia. Schmidt et al.[24] proposed that MRNF could blur retinal images and induce visual deprivation, leading to axial elongation. The amblyopia that develops in association with MRNF and myopia may be caused by form deprivation secondary to myelinated patches obscuring vision, or by optical defocus due to the high degrees of myopia.[1]

Previous studies have shown that patients with MRNF and high myopia syndrome do not respond well to treatment despite full refractive correction and intensive occlusion therapy. The presence of an abnormal macula, optic nerve dysplasia, the area and extent of myelination, the degree of myopia and anisometropia, the initial BCVA, and strabismus have been suggested as critical features determining the visual prognosis.[3,24,27,28] We evaluated the macular imaging characteristics of patients with MRNF and high myopia syndrome with the current OCT and OCTA technology to determine if there are any findings that could explain the poor prognosis of these patients. A recent meta-analysis by Gao et al.[29] showed that anisometropia and mixed amblyopia had no effect on microvessel density when compared with healthy eyes. The analysis also revealed that there was no significant difference in FAZ area between amblyopic and healthy control eyes. Based on this, we included otherwise healthy myopic eyes as a control group.

The imaging characteristics of MRNF have been reviewed recently in the literature. O'Brien et al.[25] demonstrated that peripapillary RNFL was significantly thicker in eyes with MRNF while macular thickness was within the normal range.

Naghib[23] reported a 4-year-old girl with MRNF superotemporal and inferotemporal to the macula, hypoplastic

Table 3. Comparision of the OCTA features of myelinated eyes, normal fellow eyes, and the myopic control group				
	Myelinated eyes, median (min-max) (IQR) (n=4)	**Normal fellow eyes, median (min-max) (IQR) (n=4)**	**Myopic controls, (median) (min-max) (IQR) (n=9)**	**p**
Foveal avascular zone (mm^2)	0.19 (0.16-0.29) (0.11)	0.23 (0.07-0.32) (0.21)	0.24 (0.03-0.36) (0.22)	0.98
Acircularity index	1.21 (1.12-1.81) (0.53)	1.10 (1.06-1.12) (0.05)	1.09 (1.06-1.19) (0.04)	0.02
Flow area (mm^2)	1.75 (0.85-2.47) (1.39)	0.92 (0.67-2.12) (1.17)	1.25 (0.41-1.91) (0.57)	0.35
Whole image vessel density-superficial (%)	51.05 (47.80-52.70) (4.10)	49.10 (47.70-49.70) (1.75)	47.90 (42.40-53.70) (5.75)	0.26
Foveal vessel density-superficial (%)	21.85 (10.50-53.60) (37.45)	22.30 (17.80-34.60) (14.60)	18.90 (12.10-46.00) (14.35)	0.94
Parafoveal vessel density-superficial (%)	45.60 (33.10-53.00) (17.03)	51.40 (50.10-52.70) (2.35)	49.70 (41.40-54.40) (6.40)	0.33
Perifoveal vessel density-superficial (%)	53.45 (47.50-57.70) (8.63)	49.40 (49.00-50.20) (1.00)	48.50 (43.50-54.00) (4.60)	0.11
Whole image vessel density-deep (%)	46.65 (42.70-50.30) (6.33)	43.60 (33.70-52.90) (17.40)	44.50 (31.00-53.80) (7.25)	0.61
Foveal vessel density-deep (%)	49.70 (48.30-52.80) (7.28)	39.10 (30.40-54.70) (20.93)	36.70 (29.10-57.10) (14.45)	0.50
Parafoveal vessel density-deep (%)	49.70 (48.30-52.80) (3.53)	53.00 (42.80-58.70) (14.18)	50.30 (40.40-56.90) (5.65)	0.81
Perifoveal vessel density-deep (%)	47.70 (44.90-49.50) (4.05)	44.35 (33.10-53.80) (18.90)	43.80 (30.50-54.80) (8.70)	0.42
IQR: Interquartile range (Q3-Q1), OCTA: Optical coherence tomography angiography				

disc, and high myopia. OCT of the myelinated area revealed increased thickness of the RNFL together with atrophy of the underlying retinal layers.[23] Bass et al.[2] performed SD-OCT on three patients with unilateral MRNF, optic disc hypoplasia, and axial myopia with amblyopia. All patients demonstrated either total absence or attenuation of the photoreceptor integrity line. The authors concluded that the changes demonstrated a possible structural component in a percentage of patients with reduced vision.[2] Gharai et al.[10] reported that OCT imaging of two patients with MRNF, high myopia, and small optic nerves showed a normal foveal contour and reduced retinal thickness with the same distribution as the myelination.

In our study, although all patients showed macular reflex alterations and pigmentary and positional changes in the macula, SD-OCT findings for the foveal structures were normal. Thus, macular appearance may not be a prognostic factor for visual acuity improvement if the macula is not involved by myelinated fibers. The coexistent organic pathology of the dysplastic optic nerves may be a contributing factor for poor prognosis. Choroidal thinning in high myopia was reported previously in the literature.[30] In our study, retinal thickness and SCT were compared between myelinated and contralateral normal eyes and myopic controls. Although not statistically significant, SCT was found to be thinner in both the myelinated eyes and myopic controls than in the normal fellow eyes.

In OCTA imaging, the AI was found to be higher in myelinated eyes compared to myopic controls. AI was defined as the ratio of the FAZ perimeter to the perimeter of a circle with equal area.[31] A perfectly circular FAZ has an AI of 1, with deviations from a circular shape leading to an increase in AI.[32] Changes in AI indicate irregularity in FAZ area. Piao et al.[20] recently investigated the AI of the FAZ in high myopia and found there was no significant difference in AI between high and non-high myopia. However, they also found that FAZ area positively correlated with AI in highly myopic eyes, suggesting FAZ area becomes more acircular as the degree of myopia increases.[20] In our study, the AI was similar between myopic controls and the normal fellow eyes of patients with MRNF. AI only differed significantly between myelinated eyes and myopic controls. Although the myelinated eyes were slightly more myopic, the SE values were similar statistically. Therefore, the higher AI indicating FAZ irregularity cannot be explained by the degree of myopia in our study. Higher AI may be a factor contributing to the lower visual acuity in patients with unilateral MRNF and high myopia syndrome. Changes in AI may also be related to obscuration of vascular flow signal due to MRNF in these patients. However, all of the patients in our study group showed normal foveal contour, and MRNF was not observed in the area corresponding to the FAZ. Therefore, besides the blocking effect of MRNF, significant FAZ irregularity may be an independent finding in unilateral MRNF and high myopia syndrome.

A previous study showed the density of the retinal capillary microvasculature was reduced in myopia.[33] However, in our study, we found no difference in macular VD between the three groups. OCT and OCTA imaging features are known to be affected by AL. It was shown that SD-OCT thickness measurements decrease with longer AL.[34] Additionally, it was shown that FAZ and superficial retinal VD measurements are affected by AL, and large errors in these parameters can arise in the absence of image size correction.[35,36] In our study, the AL values of the myopic control group were similar to those of the patient group. Therefore, we think that we overcame the effect of AL. Moreover, we only found a significant difference in AI in OCTA measurements, and it was shown that AI can quantify FAZ geometry without the need for AL measurements to correct for retinal magnification, unlike other OCTA metrics.[32] In light of this, our results show that significant FAZ irregularity is observed in MRNF and high myopia syndrome.

It is known the PVD incidence is increased in myopic eyes and PVD develops at a significantly younger age in highly myopic eyes.[37,38] We did not observe PVD in any of the myopic controls, whereas partial PVD was present in 67% of the eyes

with MRNF and high myopia syndrome. Our results show that PVD is more common in MRNF and high myopia syndrome than in the age-matched myopic control group. Therefore, vigilance is warranted during the follow-up of these patients, as PVD-related retinal pathologies might occur earlier in this group. Although not found to be statistically significant, choroidal thickness appears to be thinner and myopia is slightly higher in the MRNF and high myopia patient group compared to other groups, and the increased incidence of PVD may be associated with these findings.

Study Limitations

Since MRNF and high myopia syndrome is not a very common condition, we had a limited number of patients. Moreover, because of the age group of our patients, we could only perform OCTA imaging successfully in four patients. Further studies with a larger number of subjects are needed for more reliable statistical evaluations.

Conclusion

This is the first study investigating the macular imaging features of MRNF and high myopia syndrome with OCT, OCTA, and SD-EDI-OCT together. All myelinated eyes demonstrated normal foveal contour and macular structure in SD-OCT. However, in OCTA the AI was found to be higher in myelinated eyes. Normal foveal structure may implicate the role of optic nerve dysplasia and functional amblyopia in the refractory amblyopia seen in MRNF and high myopia syndrome.

Ethics

Ethics Committee Approval: Başkent University Ethics Committee (date: 25.03.2020/no: KA20/125).

Informed Consent: Obtained.

Peer-review: Externally and internally peer reviewed.

Authorship Contributions

Concept: A.S.S., S.O., İ.A., S.A.B., G.Y., Design: A.S.S., S.O., İ.A., S.A.B., G.Y., Data Collection or Processing: A.S.S., S.O., İ.A., S.A.B., G.Y., M.Y.Ç., Analysis or Interpretation: A.S.S., S.O., İ.A., S.A.B., G.Y., M.Y.Ç., Literature Search: A.S.S., S.O., S.A.B., Writing: A.S.S., S.O., İ.A., S.A.B., G.Y., M.Y.Ç.

Conflict of Interest: No conflict of interest was declared by the authors.

Financial Disclosure: The authors declared that this study received no financial support.

References

1. Tarabishy AB, Alexandrou TJ, Traboulsi EI. Syndrome of myelinated retinal nerve fibers, myopia, and amblyopia: a review. Surv Ophthalmol. 2007;52:588-596.
2. Bass SJ, Westcott J, Sherman J. OCT in a Myelinated Retinal Nerve Fiber Syndrome with Reduced Vision. Optom Vis Sci. 2016;93:1285-1291.
3. Lee MS, Gonzalez C. Unilateral peripapillary myelinated retinal nerve fibers associated with strabismus, amblyopia, and myopia. Am J Ophthalmol. 1998;125:554-556.
4. Buys Y, Enzenauer R, Crawford JS. Myelinated nerve fibers and refractory amblyopia: a case report. Ann Ophthalmol. 1993;25:353-355.
5. Straatsma BR, Heckenlively JR, Foos RY, Shahinian JK. Myelinated retinal nerve fibers associated with ipsilateral myopia, amblyopia, and strabismus. Am J Ophthalmol. 1979;88:506-510.
6. Ellis GS, Frey T, Gouterman RZ. Myelinated nerve fibers, axial myopia, and refractory amblyopia: an organic disease. J Pediatr Ophthalmol Strabismus. 1987;24:111-119.
7. Holland PM, Anderson B. Myelinated nerve fibers and severe myopia. Am J Ophthalmol. 1976;81:597-599.
8. Straatsma BR, Foos RY, Heckenlively JR, Taylor GN. Myelinated retinal nerve fibers. Am J Ophthalmol. 1981;91:25-38.
9. Moradian S, Karim S. Unilateral myelinated retinal nerve fiber layer associated with axial myopia, amblyopia and strabismus. J Ophthalmic Vis Res. 2009;4:264-265.
10. Gharai S, Prakash G, Ashok Kumar D, Jacob S, Agarwal A, Arora V. Spectral domain optical coherence tomographic characteristics of unilateral peripapillary myelinated retinal nerve fibers involving the macula. J AAPOS. 2010;14:432-434.
11. Xu K, Almeida DRP. Myelinated retinal nerve fibre, myopia, and amblyopia syndrome. Canadian journal of ophthalmology. Can J Ophthalmol. 2017;52:e127.
12. Ozates S, Teke MY. Ring-shaped myelinated retinal nerve fibers at fovea. Indian J Ophthalmol. 2017;65:630-632.
13. Di Giovanna F, Morreale Bubella D, Carita S, Morreale Bubella R, Lodato G. Retinal myelinated nerve fibers associated with macular pseudohole. J Fr Ophtalmol. 2008;31:295-298.
14. Savastano MC, Lumbroso B, Rispoli M. In Vivo Characterization of Retinal Vascularization Morphology Using Optical Coherence Tomography Angiography. Retina. 2015;35:2196-2203.
15. Lavia C, Bonnin S, Maule M, Erginay A, Tadayoni R, Gaudric A. Vessel Density of Superficial, Intermediate, and Deep Capillary Plexuses Using Optical Coherence Tomography Angiography. Retina. 2019;39:247-258.
16. Hollo G. Influence of myelinated retinal nerve fibers on retinal vessel density measurement with AngioVue OCT angiography. Int Ophthalmol. 2016;36:915-919.
17. Jampol LM, Glassman AR, Bressler NM. Comparative Effectiveness Trial for Diabetic Macular Edema: Three Comparisons for the Price of 1 Study From the Diabetic Retinopathy Clinical Research Network. JAMA Ophthalmol. 2015;133:983-984.
18. Zhang Y, Lan J, Cao D, Yang C, Yang D, Xie W, Zeng J. Microvascular changes in macula and optic nerve head after femtosecond laser-assisted LASIK: an optical coherence tomography angiography study. BMC Ophthalmol. 2020;20:107.
19. Czakó C, István L, Ecsedy M, Récsán Z, Sándor G, Benyó F, Horváth H, Papp A, Resch M, Borbándy Á, Nagy ZZ, Kovács I. The effect of image quality on the reliability of OCT angiography measurements in patients with diabetes. Int J Retina Vitreous. 2019;5:46.
20. Piao H, Guo Y, Zhang H, Sung MS, Park SW. Acircularity and circularity indexes of the foveal avascular zone in high myopia. Sci Rep. 2021;11:16808.
21. Ali BH, Logani S, Kozlov KL, Arnold AC, Bateman B. Progression of retinal nerve fiber myelination in childhood. Am J Ophthalmol. 1994;118:515-517.
22. FitzGibbon T, Nestorovski Z. Human intraretinal myelination: axon diameters and axon/myelin thickness ratios. Indian J Ophthalmol. 2013;61:567-575.
23. Naghib J. Triad of myelinated retinal nerve fibers, axial myopia and amblyopia. J Ophthalmic Vis Res. 2010;5:284-285.
24. Schmidt D, Meyer JH, Brandi-Dohrn J. Wide-spread myelinated nerve fibers of the optic disc: do they influence the development of myopia? Int Ophthalmol. 1996;20:263-268.
25. O'Brien S, Sprunger DT, Lim ME, Wang J. Myelinated Retinal Nerve Fibers in Children: OCT Imaging, Refractive Error and Vision. J Clin Exp Ophthalmol. 2016;7.
26. Oh BL, Hwang JM, Woo SJ. Myelinated nerve fiber-associated local scleral excavation and induced axial myopia. Retina. 2014;34:2028-2036.
27. Kee C, Hwang JM. Visual prognosis of amblyopia associated with myelinated retinal nerve fibers. Am J Ophthalmol. 2005;139:259-265.

28. Hittner HM, Antoszyk JH. Unilateral peripapillary myelinated nerve fibers with myopia and/or amblyopia. Arch Ophthalmol. 1987;105:943-948.
29. Gao L, Gao Y, Hong F, Zhang P, Shu X. Assessment of Foveal Avascular Zone and Macular Vascular Plexus Density in Children With Unilateral Amblyopia: A Systemic Review and Meta-Analysis. Front Pediatr. 2021;9:620565.
30. Alzaben Z, Cardona G, Zapata MA, Zaben A. Interocular Asymmetry in Choroidal Thickness and Retinal Sensitivity in High Myopia. Retina. 2018;38:1620-1628.
31. Tam J, Dhamdhere KP, Tiruveedhula P, Manzanera S, Barez S, Bearse MA Jr, Adams AJ, Roorda A. Disruption of the retinal parafoveal capillary network in type 2 diabetes before the onset of diabetic retinopathy. Invest Ophthalmol Vis Sci. 2011;52:9257-9266.
32. Krawitz BD, Mo S, Geyman LS, Agemy SA, Scripsema NK, Garcia PM, Chui TYP, Rosen RB. Acircularity index and axis ratio of the foveal avascular zone in diabetic eyes and healthy controls measured by optical coherence tomography angiography. Vision Res. 2017;139:177-186.
33. Al-Sheikh M, Phasukkijwatana N, Dolz-Marco R, Rahimi M, Iafe NA, Freund KB, Sadda SR, Sarraf D. Quantitative OCT Angiography of the Retinal Microvasculature and the Choriocapillaris in Myopic Eyes. Invest Ophthalmol Vis Sci. 2017;58:2063-2069.
34. Rock T, Bartz-Schmidt KU, Bramkamp M, Rock D. Influence of axial length on thickness measurements using spectral-domain optical coherence tomography. Invest Ophthalmol Vis Sci. 2014;55:7494-7498.
35. Sampson DM, Gong P, An D, Menghini M, Hansen A, Mackey DA, Sampson DD, Chen FK. Axial Length Variation Impacts on Superficial Retinal Vessel Density and Foveal Avascular Zone Area Measurements Using Optical Coherence Tomography Angiography. Invest Ophthalmol Vis Sci. 2017;58:3065-3072.
36. Leng Y, Tam EK, Falavarjani KG, Tsui I. Effect of Age and Myopia on Retinal Microvasculature. Ophthalmic Surg Lasers Imaging Retina. 2018;49:925-931.
37. Ng DS, Cheung CY, Luk FO, Mohamed S, Brelen ME, Yam JC, Tsang CW, Lai TY. Advances of optical coherence tomography in myopia and pathologic myopia. Eye (Lond). 2016;30:901-916.
38. Hayashi K, Manabe SI, Hirata A, Yoshimura K. Posterior Vitreous Detachment in Highly Myopic Patients. Invest Ophthalmol Vis Sci. 2020;61:33.